

## One-dimensional quantised ballistic resistors in parallel configuration

This article has been downloaded from IOPscience. Please scroll down to see the full text article.

1989 J. Phys.: Condens. Matter 1 6763

(<http://iopscience.iop.org/0953-8984/1/37/022>)

View [the table of contents for this issue](#), or go to the [journal homepage](#) for more

Download details:

IP Address: 171.66.16.96

The article was downloaded on 10/05/2010 at 20:05

Please note that [terms and conditions apply](#).

## LETTER TO THE EDITOR

# One-dimensional quantised ballistic resistors in parallel configuration

C G Smith<sup>†</sup>, M Pepper<sup>†</sup>, R Newbury<sup>†</sup>, H Ahmed<sup>†</sup>, D G Hasko<sup>†</sup>,  
D C Peacock<sup>†‡</sup>, J E F Frost<sup>†</sup>, D A Ritchie<sup>†</sup>, G A C Jones<sup>†</sup> and G Hill<sup>§</sup>

<sup>†</sup> Cavendish Laboratory, Madingley Road, Cambridge CB3 0HE, UK

<sup>§</sup> Department of Electrical Engineering, The University of Sheffield, Mappin Street, Sheffield S10 2TN, UK

Received 13 July 1989

**Abstract.** We have defined, in parallel configuration, two split gate devices  $0.3\ \mu\text{m}$  long by  $0.3\ \mu\text{m}$  wide with a centre-to-centre separation of  $0.5\ \mu\text{m}$  on a high mobility heterojunction. At low temperatures, when the phase coherence length is longer than the channel length, the conduction through each one is ballistic and shows steps in conductance of  $2e^2/h$ . If the phase coherence length is also greater than the channel separation, transport through both channels is no longer independent, but instead the channels act co-operatively, leading to coherent steps in the conductance of  $4e^2/h$ ; this can be seen even if the channels do not have the same widths. The device shows Aharonov–Bohm oscillations in resistance of amplitude 10%, arising from a current circulating via edge states through both channels, indicating that the electron wavefunction is indeed coherent through both.

Recently Wharam *et al* (1988a) and van Wees *et al* (1988) have exploited the split gate device structure developed by Thornton *et al* (1986) for the investigation of the ballistic transport of electrons. These authors fabricated a split Schottky gate device on a GaAs–AlGaAs heterojunction containing a high-mobility electron gas. By applying a negative gate voltage the width of the two-dimensional gas (2DEG) can be reduced and a transition to one dimension obtained. At low temperatures the elastic and inelastic scattering mean free paths can be several micrometres, and so, if the narrow channel is sufficiently small, electron transport becomes ballistic. Each one-dimensional (1D) subband has a conductance  $2e^2/h$ , where the factor of 2 arises from the spin degeneracy. If  $N$  1D subbands are occupied, the total conductance is  $2e^2N/h$  and if the width is continuously decreased the conductance will change by  $2e^2/h$  each time a subband is depopulated and  $N$  changes by 1.

The steps are quantised to a reasonable accuracy because there are enough two-dimensional levels in each wide region of the device which match with the levels in the channel to give a transmission probability  $T$  of 1 for each level. Subsequently Wharam *et al* (1988b) demonstrated that the total resistance of two split gates in series, separated by less than the electron mean free path, is equal to the resistance of the narrowest aperture and transport, in the absence of mode mixing, can be described by the conservation of quantum number.

<sup>‡</sup> On leave from GEC Hirst Research Centre, East Lane, Wembley, Middlesex HA9 7PP, UK.

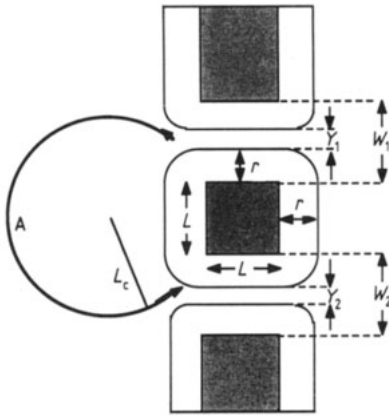


**Figure 1.** A diagram of the gate metallisation showing where it touches the underlying GaAs heterostructure. The metal is shown by the shaded area.  $r$  is the distance the electrons, in the underlying 2DEG, are depleted away from the gates. The lengths are  $L = 0.2 \mu\text{m}$  and  $W_1 = W_2 = 0.3 \mu\text{m}$ .  $Y_1$  and  $Y_2$  are the conducting widths of channel 1 and 2, while  $L_c$  is the cyclotron radius. The circle A marks a possible trajectory for an electron at a field of 0.22 T.

In this Letter we set out to investigate how the resistance of two channels, in parallel, combine when their separation is less than the elastic and phase coherence mean free paths. In this regime the electron waves should pass through both slits coherently and the double parallel channels form a coupled one-quantum system.

The device was fabricated using electron beam lithography in the manner developed by Ford *et al* (1989), which enables isolated gates to be connected using thick metal over a patterned polymethyl methacrylate (PMMA) resist layer. The PMMA acts as a dielectric so the electrons in the 2DEG are only depleted where the gate metal is in contact with the heterostructure; under the resist between the metal and the GaAs the surface states screen the 2DEG from the gate potential. The details of the underlying heterojunction are as follows: a superlattice buffer (AlAs 2.4 nm, GaAs 2.5 nm  $\times$  25) grown first on a semi-insulating substrate, followed by 1 nm of nominally undoped GaAs. On top of this 20 nm of undoped AlGaAs is grown, followed by 40 nm of AlGaAs Si-doped at  $10^{18} \text{ cm}^{-3}$  and topped by a 10 nm undoped GaAs capping layer. In this manner two narrow channels  $0.3 \mu\text{m}$  wide by  $0.2 \mu\text{m}$  long were defined with a centre to centre separation of  $0.5 \mu\text{m}$  (see figure 1). The heterostructure material has a carrier concentration,  $n$ , of  $3.4 \times 10^{11} \text{ cm}^{-2}$ , a Fermi Energy,  $E_F$ , of 12 meV and a mobility,  $\mu$ , of  $985\,000 \text{ cm}^2 \text{ V}^{-1} \text{ s}^{-1}$  at 33 mK (which implies an electron mean-free-path of more than  $5 \mu\text{m}$ ). Most of the measurements were performed on a dilution refrigerator with the sample sitting in the mixing chamber, while others were performed in a  $^3\text{He}$  cryostat. Four-terminal measurements of resistance were made using a low frequency (70 Hz) phase sensitive technique with a current of less than 1 nA.

The first set of measurements showed that sweeping the gate voltage to negative values depletes the 2DEG under the gates at 0.5 V and pinches off both channels at  $-1.42 \text{ V}$ . Figure 2 shows the first measurements of  $R$  against  $V_g$  which has steps at values of  $R = h/4e^2N$ , where  $N$  is the number of 1D subbands in one of the channels; this is consistent with both channels being the same width and shows that depopulation of the 1D subbands occurs at the same gate voltage for both channels. The last step at  $N = 1$  is not well quantised and shows two distinct sets of structure separated by 30 mV, suggesting that the two channels are not exactly the same width at pinch-off. We can estimate the difference in channel widths by exploiting the fact that the plateaux in the plot of conductance against gate voltage lie on a straight line, and by assuming the channels have a width of half the Fermi wavelength (21 nm) at  $V_g = -1.42 \text{ V}$  and a width of 300 nm at  $V_g = -0.5 \text{ V}$ . (This assumes the carrier concentration does not vary on

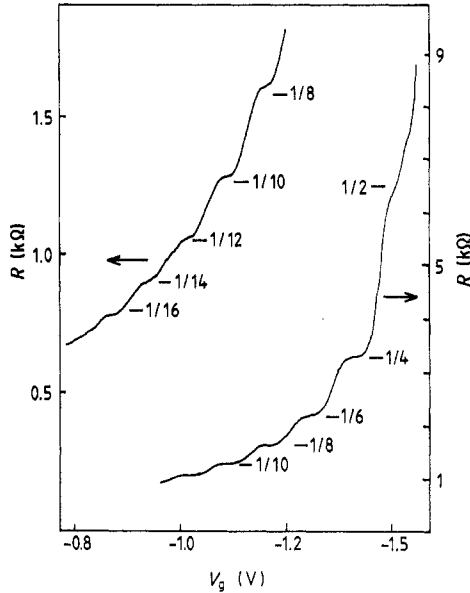


**Figure 2.** A plot of resistance against gate voltage for the first measurement. The fractions of  $h/2e^2$  are marked on the graph, showing how the resistance goes as  $(1/N)h/4e^2$  where  $N = 1, 2, 3, 4, \dots$ . It is possible to see two separate structures on the last plateau.

squeezing, which is not completely valid as Wharam *et al* (1989b) have shown, but the carrier concentration is not greatly changed when there are still 3 or more subbands in the channel). We find that the resulting conduction widths,  $Y_1$ , for one channel and  $Y_2$  for the other become  $Y_1 = W_1 - 2r$  and  $Y_2 = W_2 - 2r$ , where

$$r = 0.152 \times 10^{-6} (V_g + 0.5 \text{ V}) \text{ m.} \quad (1)$$

Here  $r$  is the distance the depletion region extends away from the gates, nominally  $W_1 = W_2 = 0.3 \mu\text{m}$ . Using equation (1) one can explain the double structure on the last plateau by assuming  $W_1 - W_2 = 10 \text{ nm}$ , which is close to the resolution limit of PMMA.

The application of a magnetic field showed that Aharonov–Bohm (AB) oscillations similar to those observed by Timp *et al* (1987) and Ford *et al* (1989) in rings could be observed each time a quantum of flux of  $h/e$  is threaded through the central dot between the two channels. This was surprising, as this area is not well defined. However, Wharam *et al* 1989, van Wees *et al* 1989 and Brown *et al* 1989 have all recently shown that if the current flows in edge states around the boundaries of a uniform system, then a ring is defined and AB oscillations are found. Figure 3 shows the resistance of the device as the magnetic field is changed at a temperature of 100 mK. The gate voltage is  $-1.195 \text{ V}$ , so each channel width is  $Y = 89 \text{ nm}$ , implying that there are between four and five subbands in each; this agrees with the value of resistance for  $B = 0 \text{ T}$  which is  $1200 \Omega$  (or  $(1/N)h/4e^2$  with  $N = 5$ ). The trace shows that until  $B = 0.22 \text{ T}$  the magnetoresistance is linear and negative; then from  $B = 0.63 \text{ T}$  to  $1.93 \text{ T}$  the resistance shows small amplitude periodic oscillations on a larger amplitude, longer period, background oscillation. The short-wavelength (AB) oscillation at its largest amplitude is 10% of the resistance at  $B = 0 \text{ T}$ . The Fourier power spectrum of figure 3 shows that there is a peak at  $60 \text{ T}^{-1}$  which implies an area for the inner dot of  $2.5 \times 10^{-13} \text{ m}^2$ , ( $500 \text{ nm}^2$ ). Assuming that the depletion width is  $r$  around the central dot, then the area will be  $(L + 2r)^2$ , and from equation (1)  $r = 1 \times 10^{-7} \text{ m}$ , so the inner area is  $400 \text{ nm}^2$ . These results can be explained by recognising that it is the magnetic edge states encircling the central dot that define

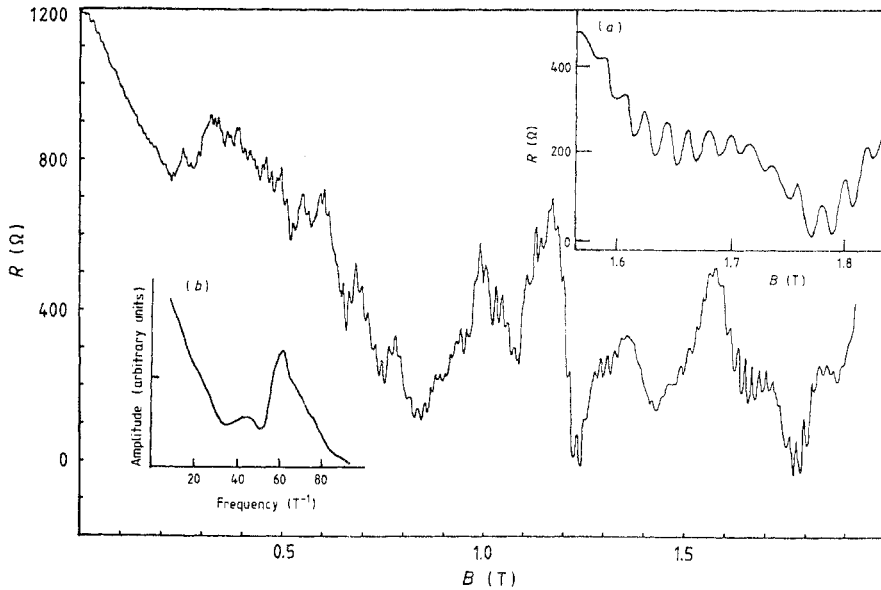


**Figure 3.** The resistance plotted against magnetic field for  $V_g = -1.195$  V. Inset (a) shows a blow-up of the trace above 1.6 T showing the Aharonov-Bohm oscillations. Inset (b) shows the Fourier power spectrum of the whole magnetoresistance trace showing a peak at  $60 \text{ T}^{-1}$ .

the conducting path. At  $B = 0.22$  T the cyclotron orbit, given by  $L_c = (\hbar k_F / 2\pi e B \sqrt{2})$ , is 311 nm, where  $k_F$  is the Fermi wavevector. This is the value of  $B$  for which a large percentage of the electrons leaving one channel are focused by the field into the other (see figure 1). From  $B = 0.22$  T to  $B = 0.63$  T there are small AB oscillations which slowly increase in period as the cyclotron orbit shrinks, so at the higher fields  $L_c = 111$  nm. The conducting path on average has a width  $L_c$ , hence the accuracy of the AB effect increases with field, the accuracy is given by:

$$2L_c(L + L + 2r)/(L + 2r)^2. \quad (2)$$

If we calculate the AB area using the last ten oscillations from  $B = 1.6$  T the area obtained is  $2.3 \times 10^{-9} \text{ cm}^2$  which is within 20% of that calculated from equation (1), the error estimated from equation (2) being 30%.

Another method of investigating the AB effect is to hold the magnetic field constant and change the flux by changing the area. This can be done by sweeping the gate voltage, which alters  $r$  and thus the area of the central dot. In figure 4(a) the oscillations observed on the plateaux as the gate voltage is changed are plotted for several values of magnetic field. A change of one flux quantum in the dot occurs when the area changes by  $dA = h/eB$ , leading to oscillations in the resistance with  $V_g$ , but

$$A = (L + 2r)^2 \quad dA/dr = 4L + 8r \quad (3)$$

and

$$dA/dV_g = (4L + 8r) dr/dV_g. \quad (4)$$

Thus by inserting the differential of equation (1) into equation (4) one obtains

$$dA/dV_g = (4L + 8r)0.152 \times 10^{-6} \text{ m}^2 \text{ V}^{-1} \quad (5)$$

so we can compare the  $dA/dV_g$  calculated from equation (5) with the measurements in

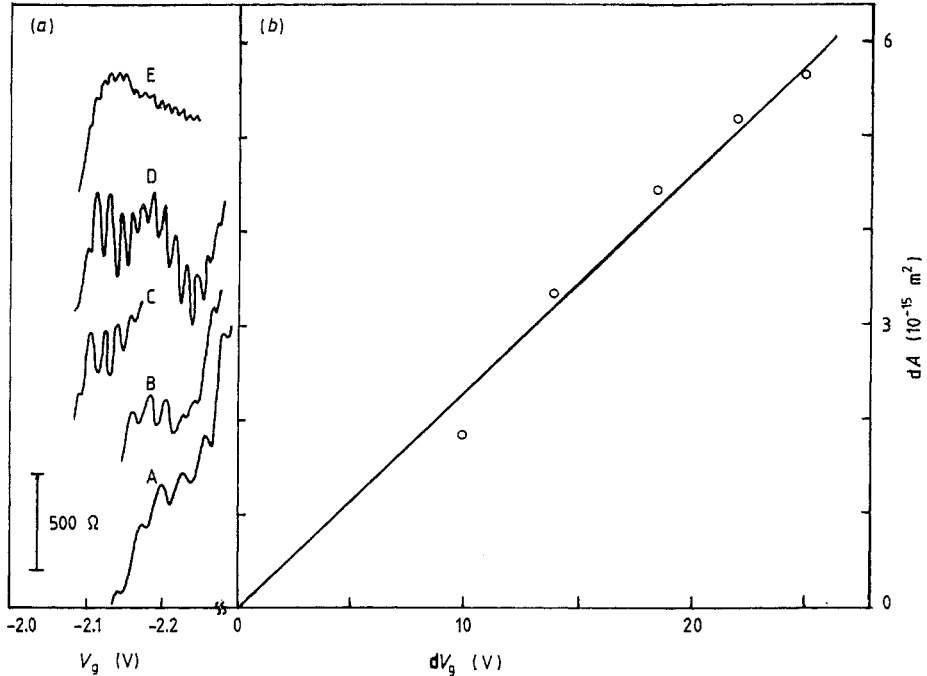


**Figure 4.** (a) The oscillations in resistance observed as the gate voltage is swept for five different values of magnetic field. Each trace is displaced by  $500 \Omega$  from the previous one and corresponds to the  $h/8e^2$  plateau in resistance. Curve A,  $B = 0.715 \text{ T}$ ; curve B,  $B = 0.8 \text{ T}$ ; curve C,  $B = 0.93 \text{ T}$ ; curve D,  $B = 1.24 \text{ T}$ ; curve E,  $B = 2.21 \text{ T}$ . (b) A plot of  $dA$ , the change in area at a field  $B$  required to allow one more flux quantum to enter the central dot, against  $dV_g$  the period in gate voltage of the resulting oscillations. The slope  $dA/dV_g = 2.31 \times 10^{-13} \text{ m}^2 \text{ V}^{-1}$ .

figure 4(a). Figure 4(b) shows a plot of the measured  $dV_g$  against  $dA$  showing a straight line, the inverse slope of which is  $2.3 \times 10^{-13} \text{ m}^2 \text{ V}^{-1}$ . That calculated from equation (5) is  $2.43 \times 10^{-13} \text{ m}^2 \text{ V}^{-1}$ , which is in very good agreement.

Over the period of measurement of several weeks the resistance against gate voltage curves showed plateaux at different values of conductance consistent with one channel pinching off at a less negative voltage. This drift in characteristic probably arises from electronic trapping in the AlGaAs above one split gate either causing the channel to be narrower or to have a smaller carrier concentration. Such a drift is commonly observed in low-temperature studies of semiconductor structures and can be put to effective use. Figure 5 shows the variation of conductance against gate voltage for samples measured on four different occasions. The top curve (marked A) was obtained on the first measurement when both channels are very nearly the same width. Surprisingly, the plateaux lie on a straight line with an average gate voltage separation of  $79 \text{ mV}$  and an average plateaux width of  $30 \text{ mV}$ . The next line (marked B) is displaced  $20 \text{ mV}$  to the left for clarity and shows the conductance versus gate voltage relation obtained on the following day. On this occasion there is a step at  $2e^2/h$  before it increases by steps in units of  $4e^2/h$ . The average separation of plateaux is still  $79 \text{ mV}$  so this first plateau at  $2e^2/h$  must occur when one channel is closed and the other has one subband within it. Because the plateaux change by units of  $4e^2/h$  we must either assume that there are  $N$  1D subbands

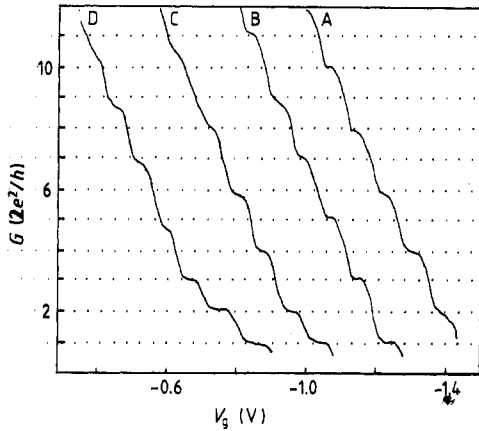


**Figure 5.** A plot of conductance  $G$  against gate voltage taken on four different occasions. Curve A was the first measurement and it shows the conductance going in steps of  $4e^2/h$ . Curve B has been displaced by 0.2 V to the left for clarity and shows the situation on the following day. Now there is a step of  $2e^2/h$  followed by steps of  $4e^2/h$ . Curve C was taken another day later and it has been displaced a further 0.2 V to the left for clarity. Now there are two steps of  $2e^2/h$  before it goes in steps of  $4e^2/h$ . Finally, curve D was taken one month later and shows that there are now three steps of  $2e^2/h$  before the  $4e^2/h$  steps come in. Again this curve is displaced a further 0.2 V to the left. The estimated differences between the channel widths are  $5.5 \times 10^{-9}$  m (curve A),  $11 \times 10^{-9}$  m (curve B),  $32 \times 10^{-9}$  m (curve C) and  $45 \times 10^{-9}$  m (curve D).

in one channel and  $N + 1$  subbands in the other and that they disappear at the same value of gate voltage, or we must assume that there is a cooperative effect occurring so that the subbands in the separate channels depopulate together. Curve C was taken another day later when the channels had changed further. Now there is a plateau at  $2e^2/h$ ,  $4e^2/h$  and then at intervals of  $4e^2/h$ , indicating that there are  $N$  levels in one channel when there are  $N + 2$  levels in the other. Again the levels appear to line up. Finally curve D shows the situation after one month where there are  $N$  levels on one side and  $N + 3$  levels on the other, with steps at 2, 4, and  $6e^2/h$  followed by steps at intervals of  $4e^2/h$ . Again the levels appear to line up. These results can be explained by assuming that over the measurement period one channel pinches off at  $-1.55 \text{ V} \pm 0.45 \text{ mV}$ , and the other one progressively pinches off at less negative gate voltages, until the last measurement when it pinches off 185 mV earlier. This corresponds to a difference in width of approximately 56 nm.

If we assume that the plateaux of the individual channels are completely periodic in gate voltage and that to observe a plateau in the combined system they must overlap by 20%, then the probability that they coincide is 58%. But we have measured the system on five different occasions when the comparative widths of the two channels have changed, and on every occasion the plateaux line up. The probability of this happening is only 10%. From the mobility and the  $\Delta B$  measurement we have shown that the electron inelastic and elastic mean free paths are much greater than the channel separation, so the device must be considered as a single quantum system and this has consequences which we now discuss.

The principal result of the experiment is that when the channels are within a phase coherence length, they form a coupled system in which subbands in both depopulate together so causing the plateaux regions to lock together and jump by  $4e^2/h$ . Thus, a particular channel will depopulate a level at a gate voltage, or width, which it would not when acting as a single system. In order for this to occur, the carrier concentration within each channel must change when they are coupled. We suggest that this violation of local charge neutrality can occur, if sufficiently small, due to the minimisation of the energy of the coupled system. We now give a simple argument in support of this suggestion.

We identify two channels 1 and 2 which have  $n_1$  and  $n_2$  carriers when acting separately, Fermi energies  $E_{F1}$  and  $E_{F2}$  and  $i$  and  $j$  occupied subbands, respectively.

The total electron kinetic energy is  $E$  and  $E_1$  and  $E_2$  for the two channels. We assume that carriers transfer from one channel to the other in order to minimise the total energy. The appropriate condition for stability is

$$\delta E / \delta n_1 = 0 \quad (6)$$

and

$$\delta E_1 / \delta n_1 = \delta E_2 / \delta n_2.$$

Neglecting the factor of  $1/3$ , we can write  $E_1$  as

$$E_1 = E_{Fi} + (E_{Fi} + E') + (E_{Fi} + E'') + \dots$$

where  $E_{Fi}$  is the Fermi energy in the highest occupied ( $i$ th) subband measured with respect to the bottom of the subband,  $E'$  is the energy difference between the  $i$  and the  $(i-1)$  subbands,  $E''$  is the energy difference between the  $i$  and the  $(i-2)$  subbands, and so on. Thus

$$\delta E_1 / \delta n_1 = i \delta E_{Fi} / \delta n_1. \quad (7)$$

As  $E_{Fi} \rightarrow 0$ , which is the situation of relevance here, the density of states in this subband tends to infinity and, hence,  $\delta n_i \approx \delta n_1$ . Therefore, provided the  $i$  and  $j$  subbands dominate the densities of states of their respective channels

$$\delta E_1 / \delta n_1 = i \delta E_{Fi} / \delta n_i$$

as  $n_i = C E_{Fi}^{1/2}$  where  $C$  is a constant. Thus

$$\delta E_1 / \delta n_1 \approx (2i/C) E_{Fi}^{1/2}. \quad (8)$$

Similarly

$$\delta E_2 / \delta n_2 \approx (2j/C) E_{Fj}^{1/2} \quad (9)$$

and  $i E_{Fi}^{1/2} = j E_{Fj}^{1/2}$  becomes the condition for the minimisation of energy. Thus  $E_{Fi}$  and  $E_{Fj}$  go to zero together as  $i \rightarrow i-1$  and  $j \rightarrow j-1$ , and the resultant coupling of the two channels produces the locking of the jump in the quantised conductance.

This argument will increasingly break down as the separation of the channel increases to become greater than the phase coherence lengths, as we have observed, as well as when the disparity in channel width, and transfer of charge, between the channels becomes significant. This decoupling will tend to occur when the channel widths are narrow, and the number of occupied levels are few, as can be seen in figure 2 when the  $N=1$  subband becomes decoupled and the individual channels show separate structure. These experiments have been repeated with a greater channel separation of  $1 \mu\text{m}$ . We did not see Aharonov-Bohm oscillations and the conductance characteristics were of two channels retaining individuality with ill-defined plateaux appearing at non-quantised values of conductance. Further details will be published shortly. Finally we note that phase coherence does not enter our simple filling argument. Possibly the electron-electron interaction is involved in a subtler way.

This work was supported by SERC, and in part by the EEC under the auspices of the ESPRIT Basic Research Action, 3043. We are grateful for much assistance and advice received from the III-V Semiconductor Centre at Sheffield University.



**References**

- Brown R, Smith C G, Pepper M, Ahmed H, Frost J E F, Hasko D G, Peacock D C, Ritchie D A and Jones G A C 1989 *J. Phys.: Condens. Matter* at press
- Büttiker M 1988 *IBM J. Res. Dev.* **32** 317
- Ford C J B, Thornton T J, Newbury N, Pepper M, Ahmed H, Peacock D C, Ritchie D A, Frost J E F and Jones G A C 1989 *Appl. Phys. Lett.* **54** 21
- Smith C G, Pepper M, Ahmed H, Frost J E F, Hasko D G, Newbury R, Peacock D C, Ritchie D A and Jones G A C 1989 *J. Phys.: Condens. Matter* at press.
- Smith C G, Pepper M, Ahmed H, Frost J E F, Hasko D G, Peacock D C, Ritchie D A and Jones G A C 1988 *J. Phys. C: Solid State Phys.* **21** L893-8
- Thornton T J, Pepper M, Ahmed H, Andrews D and Davies G J 1986 *Phys. Rev. Lett.* **56** 1198
- Timp G, Chang A M, Cunningham J E, Chang T Y, Mankiewich P, Behringer R and Howard R E 1987 *Phys. Rev. Lett.* **58** 2814
- van Wees B J, Kouwenhoven L P, Harmans C J P, Williamson J G, Timmering C E, Broekaart M E J, Foxon C T and Harris J J 1989 *Phys. Rev. Lett.* **62** 2523
- van Wees B J, van Houten H, Beenakker C W J, Williamson J G, Kouwenhoven L P, van der Marel D and Foxon C T 1988 *Phys. Rev. Lett.* **60** 848
- Wharam D A, Thornton T J, Newbury R, Pepper M, Ahmed H, Frost J E F, Hasko D G, Peacock D C, Ritchie D A and Jones G A C 1988a *J. Phys. C: Solid State Phys.* **21** L209
- Wharam D A, Pepper M, Ahmed H, Frost J E F, Hasko D G, Peacock D C, Ritchie D A and Jones G A C 1988b *J. Phys. C: Solid State Phys.* **21** L887
- Wharam D A, Pepper M, Newbury R, Ahmed H, Hasko D G, Peacock D C, Frost J E F, Ritchie D A and Jones G A C 1989a *J. Phys.: Condens. Matter* **1** 3369
- Wharam D A, Ekenburg U, Pepper M, Hasko D G, Ahmed H, Frost J E F, Ritchie D A, Peacock D C and Jones G A C 1989b *Phys. Rev.* **39** 6283